

Cathodoluminescence spectroscopy of ambipolar diffusion in (Al,Ga)As barriers and capture of nonequilibrium carriers in GaAs quantum wells

K. Fujiwara,^{1,a)} U. Jahn,² and H. T. Grahn²

¹Kyushu Institute of Technology, Tobata, Kitakyushu 804-8550, Japan

²Paul-Drude-Institute for Solid State Electronics, Hausvogteiplatz 5-7, 10117 Berlin, Germany

(Received 19 May 2008; accepted 20 August 2008; published online 8 September 2008)

Ambipolar vertical diffusion of carriers generated in an $\text{Al}_{0.3}\text{Ga}_{0.7}\text{As}$ barrier is investigated by cathodoluminescence (CL) spectroscopy in a system containing a sequence of GaAs-based quantum wells (QWs). The intensity distribution of the CL line scan exhibits a single exponential decay for the first QW of the sequence, reflecting a pure diffusion-limited transport. However, the CL line scans of the second, third, and fourth QWs are governed by diffusion only for large separations between the electron beam and the corresponding QW. For smaller distances, the CL intensity distribution is significantly influenced by the carrier capture into the intervening QWs. © 2008 American Institute of Physics. [DOI: 10.1063/1.2980021]

In addition to the drift motion, the diffusion of carriers is one of the most important physical concepts in semiconductors for device applications. The corresponding measurement method dates back to the Haynes–Shockley experiment.¹ The relationship connecting the diffusion constant D and the mobility μ is well known as the Einstein relation given by the equation $D/\mu = k_B T/e$. Previously, many techniques have been applied to characterize D and μ .^{2,3} For example, Zarem *et al.*² used cathodoluminescence (CL) for determining the carrier diffusion length $L = (D\tau)^{1/2}$, where τ denotes the carrier lifetime, in bulk semiconductor materials of GaAs and (Al,Ga)As as well as GaAs quantum wells (QWs) in the lateral direction because of the simplicity of principle. They used a focused electron beam to generate carriers in a very small area of the sample. After diffusing across the metal masked region, the carriers (electrons and holes) are detected by radiative recombination in the unmasked region. When the distance (x) between the small excitation spot and the detection boundary is increased, the number of diffused carriers is decreased so that the detected CL intensity is reduced, as characterized by the exponential decay function $I_{\text{CL}}(x) = I_0 \exp(-x/L)$. Thus, the diffusion length L can be determined if $I_{\text{CL}}(x)$ is plotted on a logarithmic scale as a function of electron beam position. As the growth technology of sophisticated heterojunction materials advances, controlling the structure on a nanometer scale dimension, the vertical motion of carriers plays an important role in heterostructure devices, where the carriers move only over a distance shorter than the diffusion length.

In this paper, the vertical transport of carriers in a separate-confinement heterostructure (SCH) is investigated by CL spectroscopy with a high spatial resolution. By measuring spectrally discriminated CL intensities from various recombination sites, which are progressively distant from the excitation position, we observe a crossover from the diffusion-limited transport to the onset of vertical capture of nonequilibrium carriers within QWs acting as carrier traps.

The physical principle of our experiment is similar to the previous one,² but here we fully utilize different trapping sites located in a SCH as a spectrally discriminated marker (detector) of the carrier movement. For our experiments, we used a sample consisting of three QWs differing in well thickness, grown on an undoped GaAs (100) substrate by molecular-beam epitaxy with growth interruption at the well-layer interfaces.^{4–7} The nominal widths of the GaAs QWs, which are separated from each other by 36 nm thick $\text{Al}_{0.2}\text{Ga}_{0.8}\text{As}$ inner barriers, amount to 7.8 nm (QW2), 5.5 nm (QW3), and 3.5 nm (QW4) starting from the substrate side. The three QWs and the two inner barriers are embedded in a pair of 72 nm thick $\text{Al}_{0.2}\text{Ga}_{0.8}\text{As}$ barriers. This whole structure is additionally confined by 0.19 μm (surface side) and 0.43 μm (substrate side) $\text{Al}_{0.3}\text{Ga}_{0.7}\text{As}$ outer barriers, forming a SCH configuration. A high-resolution cross-sectional image of the cleaved sample taken by scanning electron microscopy (SEM) is shown in Fig. 1. The three QWs can be clearly resolved, demonstrating the high resolution of our SEM system. In Fig. 1, an unintentionally introduced interface layer (IL) with a broad QW-like profile is additionally seen between the bottom $\text{Al}_{0.2}\text{Ga}_{0.8}\text{As}$

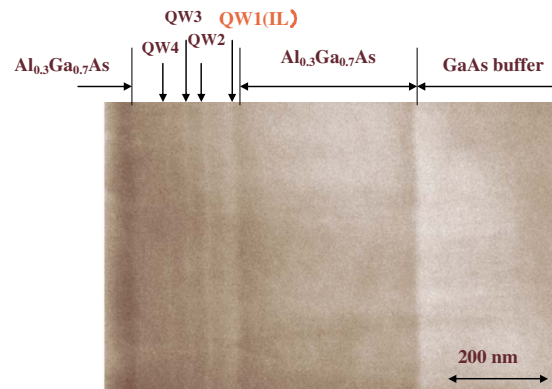


FIG. 1. (Color online) Cross-sectional SEM image of the cleaved sample, including regions of the top (left) and bottom (right) $\text{Al}_{0.3}\text{Ga}_{0.7}\text{As}$ barriers, the GaAs buffer, and the QW layers. Note that the three QWs as well as the IL formed between the top and bottom $\text{Al}_{0.3}\text{Ga}_{0.7}\text{As}$ layers are resolved in the SEM image.

^{a)}Author to whom correspondence should be addressed. Electronic mail: fujiwara@ele.kyutech.ac.jp.

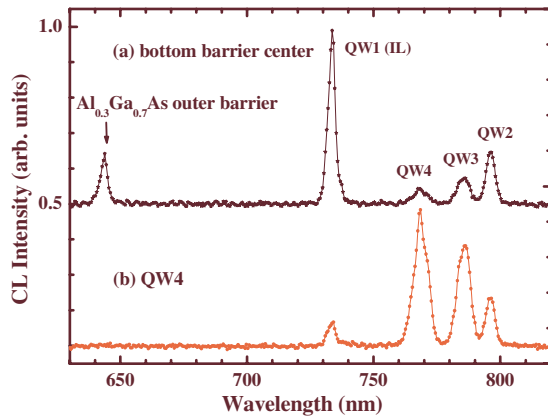


FIG. 2. (Color online) CL spectra measured on the cleaved edge of the sample at 6 K. For (a) and (b), the electron beam positions have been set to the center of the bottom $\text{Al}_{0.3}\text{Ga}_{0.7}\text{As}$ barrier and to the QW4 layer, respectively.

and $\text{Al}_{0.3}\text{Ga}_{0.7}\text{As}$ layers, which is formed due to an Al cell temperature overshoot. Coming from the substrate side, we consider this IL layer as QW1 acting as a carrier trap. We make use of this IL as a local detector to monitor the carrier motion at the edge of the thick $\text{Al}_{0.3}\text{Ga}_{0.7}\text{As}$ bottom barrier, where carriers can diffuse. Spatially resolved cross-sectional CL spectroscopy was performed on the cleaved edge of the sample in the SEM system at 6 K, using an electron beam energy of 3 keV and a beam current of 0.1 nA. A spectrometer with a focal length of 0.3 m and a cooled charge coupled device (CCD) array detector were used to disperse and detect the CL signal, respectively. The spatial resolution of the CL measurement amounts to about 50 nm.

For the CL spectra shown in Figs. 2(a) and 2(b), the electron beam is focused at the center of the bottom barrier and at the position of QW4, respectively. In the wavelength range between 750 and 810 nm, three exciton bands due to QW2–QW4 are observed, in agreement with our previous studies.^{4,7,8} In Fig. 2(a), the CL peak centered at about 640 nm can be assigned to the exciton recombination in the $\text{Al}_{0.3}\text{Ga}_{0.7}\text{As}$ barrier. A strong CL peak observed at 733 nm is attributed to the IL layer (QW1), whose presence is also confirmed using cross-sectional transmission electron microscopy. When the bottom $\text{Al}_{0.3}\text{Ga}_{0.7}\text{As}$ barrier is excited [Fig. 2(a)], the CL intensity of the IL is highest, and the CL intensities of QW2–QW4 decrease progressively with increasing distance from the bottom barrier edge. In Fig. 2(b), however, the CL intensity of the IL is lowest, and a reverse tendency of the CL intensities of QW2–QW4 is clearly observed. This means that the carrier capture by the QWs strongly depends on the position of the electron beam relative to the recombination site.

A series of spot CL spectra for varying excitation positions (with a step length of $0.017 \mu\text{m}$) was recorded by moving the electron beam position across the heterostructure along the cleaved edge of the sample (vertical CL line scan). Figure 3 shows the logarithm of the integrated CL intensities I_{CL} of the three emission bands due to QW2–QW4 as well as the additional emission due to QW1 (IL) at 6 K as a function of electron beam position. Since the CCD detector does not allow the acquisition of the complete spectral range in one shot, two line scans along the same pathway were performed to cover the three QW spectra in the first scan and the spectra of QW4 and QW1 (IL) in the second scan. Both profiles are

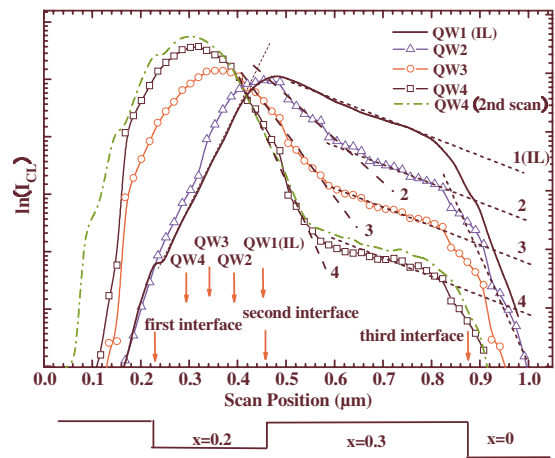


FIG. 3. (Color online) Cross-sectional distributions of the logarithm of the CL intensity measured on the cleaved edge of the sample as a function of beam position for the four bands at 6 K. The dashed lines are guides to the eye.

then superimposed, where the CL intensity distribution of QW4 is used to exactly calibrate both pathways. The CL intensities of the $n=1$ exciton states of QW4, QW3, and QW2 exhibit successive maxima as the scan position moves towards the substrate exactly in order of the growth sequence and at the expected position. Note that the CL intensity of QW1 (IL) is highest when excited near the IL position.

In addition, QW1 (IL) shows a single exponential decay as the excitation position moves away from the IL layer, indicating a diffusion-limited process operative for the ambipolar carrier transport from the excitation position within the bottom $\text{Al}_{0.3}\text{Ga}_{0.7}\text{As}$ layer towards the IL recombination site. The rate equation for the occupation number $N_0(x, t)$ of electron-hole pairs generated in the bulk $\text{Al}_{0.3}\text{Ga}_{0.7}\text{As}$ layer is given by

$$\frac{\partial N_0}{\partial t} = G\delta(x-x_0) + D\frac{d^2 N_0}{dx^2} - \frac{N_0}{\tau}, \quad (1)$$

where $G\delta(x-x_0)$ is the generation delta function at position x relative to the recombination site at x_0 and τ is the lifetime of carriers in $\text{Al}_{0.3}\text{Ga}_{0.7}\text{As}$. In steady state, the solution is given by the characteristic function $\exp[-(x-x_0)/L]$. Therefore, from the exponential decay of the CL intensity of QW1 (IL) in Fig. 3, we deduce a diffusion length $L=(D\tau)^{1/2}$ of $0.31 \mu\text{m}$. Taking the mobilities for electrons and heavy holes from the literature,⁹ a carrier lifetime value of $\tau=5$ ns is estimated, in reasonable agreement with the previous study.² Within the bottom barrier region distant from the IL boundary (in the $0.6\text{--}0.8 \mu\text{m}$ region in Fig. 3), the CL intensities of QW2–QW4 show the same diffusion-limited exponential decay, as guided by the dashed lines, although their absolute CL intensity significantly decreases. The CL intensity of QW4 exhibits the smallest value among the four QW bands since the QW4 position is located farthest from the edge of the bottom $\text{Al}_{0.3}\text{Ga}_{0.7}\text{As}$ barrier. This result indicates that the capture rate of the carriers by QW4 after diffusion from the bottom $\text{Al}_{0.3}\text{Ga}_{0.7}\text{As}$ barrier is the smallest (the capture time is longest). For a small distance between the excitation spot and the IL position, the CL intensities of QW2–QW4 significantly increase due to the onset of direct capture. The exponential slope of the CL intensity distribution of QW2 is larger as compared with the one for a large distance. This

means that the effective carrier diffusion length measured at QW2 is shorter than the value of L obtained for the detection at the IL position because of the presence of the intervening QW1 (IL) trapping site. Taking this additional trapping rate into account, the rate equation for the occupation number N in $\text{Al}_{0.3}\text{Ga}_{0.7}\text{As}$ is modified and given by

$$\frac{\partial N}{\partial t} = G\delta(x - x_0) + D\frac{d^2N}{dx^2} - \frac{N}{\tau} - \sum_{i=1}^3 \frac{N}{\tau_{+i}}, \quad (2)$$

where τ_{+i} ($i=1$) is a capture time due to the additional IL trap. Then, under steady state conditions, the effective diffusion length L_{eff} is reduced because of the reduction in the effective lifetime τ_e ($1/\tau_e = 1/\tau + 1/\tau_{+1}$). If the number of intervening traps increases from 2 [$i=1$ and 2 for QW1 (IL) and QW2] for QW3 to 3 [$i=1-3$ for QW1 (IL), QW2, and QW3] for QW4, the CL intensity distribution observed in Fig. 3 exhibits an increasing exponential slope within the region near the interface boundary. As a result, the effective diffusion length becomes shorter and shorter. From the experimental CL intensity distribution of QW2–QW4, reduced diffusion lengths of 0.13, 0.09, and 0.05 μm , respectively, are obtained, where the last value (QW4) is already mainly limited by the spatial resolution due to the electron scattering within the material. Note that near the bottom boundary with the GaAs buffer (within the position range between 0.8 and 1 μm), the slope of the CL intensity distributions is again large and on the same order of magnitude for the different QWs. This observation can be explained by the potential barrier at the GaAs/ $\text{Al}_{0.3}\text{Ga}_{0.7}\text{As}$ heterointerface, preventing diffusion of carriers, which are generated within the GaAs buffer layer, towards the QW region. This slope basically reflects the spatial resolution of the CL measurement. It is also important to note that the CL intensity distribution of QW1 (IL) is quite asymmetric with respect to the IL boundary (0.45 μm position). This can now be easily understood by the reduction in the effective diffusion length (L_{eff}

$\sim 0.05 \mu\text{m}$) within the region between 0.25 and 0.4 μm due to the intervening trap sites (QW4, QW3, and QW2) for the carriers to arrive at the IL recombination site.

In summary, CL intensity distributions due to exciton radiative recombination have been investigated at the cross section of a SCH consisting of GaAs-based QWs with different thicknesses with a high spatial resolution. Measurements of spectrally discriminated CL intensities originating from the various QWs allow to observe how the respective CL intensities are influenced by the excitation position within the barrier region. A diffusion-limited transport is clearly observed in the CL intensity distribution, when there is no intervening trapping site. However, the capture of generated carriers into intervening trapping sites between the excitation and recombination positions significantly reduces the effective diffusion length. We thus find that the ambipolar carrier transport by diffusion strongly depends on the traversing pathway.

The authors would like to thank Esperanza Luna and Achim Trampert for transmission electron microscopy on the investigated sample.

¹J. R. Haynes and W. Shockley, *Phys. Rev.* **81**, 835 (1951).

²H. A. Zarem, P. C. Sercel, J. A. Lebens, L. E. Eng, A. Yariv, and K. J. Vahala, *Appl. Phys. Lett.* **55**, 1647 (1989).

³A. Fiore, M. Rossetti, B. Alloing, C. Paranthoen, J. X. Chen, L. Geelhaar, and H. Riechert, *Phys. Rev. B* **70**, 205311 (2004) and references therein.

⁴K. Fujiwara, M. Ohe, M. Matsuo, T. Nogami, H. T. Grahn, and K. H. Ploog, *Inst. Phys. Conf. Ser.* **166**, 103 (2000).

⁵U. Jahn, K. Fujiwara, J. Menniger, R. Hey, and H. T. Grahn, *J. Appl. Phys.* **77**, 1211 (1995).

⁶U. Jahn, K. Fujiwara, R. Hey, J. Kastrop, H. T. Grahn, and J. Menniger, *J. Cryst. Growth* **150**, 43 (1995).

⁷L. Schrottke, H. T. Grahn, and K. Fujiwara, *Phys. Rev. B* **56**, 13321 (1997).

⁸K. Fujiwara, H. T. Grahn, L. Schrottke, and K. H. Ploog, in *Proceedings of the 25th International Conference on the Physics of Semiconductors*, edited by N. Miura and T. Ando (Springer, Berlin, 2001), pp. 627–628.

⁹S. Adachi, *J. Appl. Phys.* **58**, R1 (1985).